JOURNAL OF THEORETICAL
AND APPLIED MECHANICS
43, 4, pp. 875-892, Warsaw 2005

DAMPING OF VIBRATIONS IN A POWER TRANSMISSION SYSTEM CONTAINING A FRICTION CLUTCH

Zbigniew Skup

Institute of Machine Design Fundamentals, Warsaw University of Technology
e-mail: zskup@ipbm.simr.pw.edu.pl

This paper presents a theoretical study of the process of damping of non-linear vibrations in a three-mass model of a power transmission system with a multi-disc flexible friction clutch switched on and off electromagnetically. Steady-state motion of the system is subject to harmonic excitation. The problem is considered on the assumption of a uniform unit pressure distribution between the contacting surfaces of the cooperating friction discs. Structural friction, small relative sliding of the clutch discs and linear viscotic damping have also been taken into account. In the case of sliding, the friction coefficient is not constant but depends on the relative angular velocity of slowly sliding discs. The aim of the analysis is to assess the influence of geometric parameters of the system, its external load, unit pressure, viscotic damping on resonance curves and phase shift angle of steady-state vibrations. The equations of motion of the examined system are solved by means of the slowly varying parameters (Van der Pol) method and digital simulation.

Key words: non-linear vibrations, viscotic damping, friction clutch, structural friction, hysteresis loop

1. Introduction

Friction clutches of usual design, including single and multi-disc systems, have an important property of damping torsional vibrations as a result of micro and macro slip between torsionally flexible discs. The sliding effect in the elastic range of the material of cooperating elements is called the structural friction. This phenomenon is well know and referred to as a structural hysteresis loop (see Godman and Klamp, 1956; Pian, 1957 or Caughey, 1960 for early studies). In the Polish literature, an overview of structural friction problems with applications can be found in the works by Osiński (1986, 1998), Giergiel (1990), Gałkowski (1981), Kosior and Wróbel (1986). Structural friction is a natural source of damping present in every real device. In friction clutches, the magnitude of dissipation can be controlled in such a way that the best dynamic properties of the entire transmission system are obtained. Nominal driving or resistance torques of such systems are usually disturbed by additional forces of a periodical or random nature.

From the point of view of clutch design, it is important to establish a relation between the external driving load and corresponding torsional motion of the transmission system. Therefore, a dynamic analysis based on more advanced models is necessary. During the past two decades, attention was mainly focused on dynamical analysis of systems with structural friction, using relatively simple models of both the stick-slip process and the mechanical system. More advanced stick-slip models were developed based mainly on finite elements (see Buczkowski and Kleiber, 1997; Buczkowski, 1999; Grudziński *et al.*, 1992; Pietrzakowski, 1986; Zboiński and Ostachowicz, 1997). A number of papers devoted to various dynamical problems of friction clutches was presented by Skup (1991a,b, 1998, 2001, 2003, 2004), who developed an analytic description of the dynamic friction torque in a multi-disc clutch with torsionally flexible discs and shafts, and applied this result to solve vibration problems in transmission systems related to various excitation loads.

The relation between an external load and relative angular displacements of discs is of the fundamental importance for the design of friction clutches and their proper selection for particular engine-machine systems.

The degree of energy dissipation in a power transmission system can be controlled in order to obtain the best dynamical properties of the whole system. The traditional professional literature treats frictional torsion dampers, frictional clutches and brakes as joints of rigid bodies. Therefore, the effect of natural damping has been neglected.

The author of this paper takes into consideration the elasticity of the material of cooperating elements in a friction clutch. The problem is investigated on the assumption of a uniform distribution pressures, non-uniform friction coefficient and linear viscous damping. The problem of deriving a precise mathematical description of the structural friction is very complicated because of the complexity of the friction phenomenon as well as difficulties in describing the stress and strain states present in the sliding zone. Therefore, the mathematical description is based on many simplifications.

The assumptions concerning the properties of the material and friction forces are the same as in the classical theory of elasticity and structural friction theory. In the case when friction forces are smaller than applied loadings, there is a macro-slide (a kinetic coefficient of friction) between the cooperating elements. Such a phenomenon is accompanied by the occurrence of friction forces. Studies which have been conducted so far by the author in the domain of mechanical systems with structural friction were based on the assumption that there was no sliding between the cooperating elements (in the case of a static coefficient of friction, for micro-sliding). The phenomena of structural friction and macro-slip appear simultaneously during engagement or overloading the damper.

Characteristics of friction are based also on the experimental research presented by Grudziński *et al.* (1992), Kołacin (1971), Popp and Stelter (1990), Skup (1998). Most of the work has been restricted to the analysis of a one-degree-of-freedom system.

2. Equations of motion of the mechanical system

We assume a three-mass model of a mechanical system which consists of an engine (E), friction clutch (C), reduced mass (RM) and a working machine (WM), as shown in Fig. 1. Structural friction occurs between the cooperating surfaces of discs of a friction clutch (C).

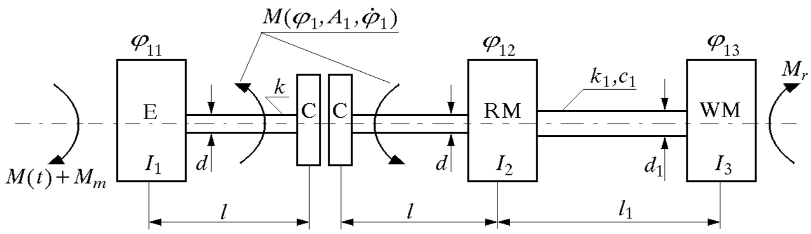

Fig. 1. Physical model of the considered power transmission system

Therefore, equations of motion of the considered system may be written down as follows

$$\begin{aligned}
&I_1\ddot{\varphi}_{11} + M_z = M(t) + M_m \\
&I_2\ddot{\varphi}_{12} - M_z + k_1(\varphi_{12} - \varphi_{13}) + c_1(\dot{\varphi}_{12} - \dot{\varphi}_{13}) = 0 \\
&I_3\ddot{\varphi}_{13} - k_1(\varphi_{12} - \varphi_{13}) - c_1(\dot{\varphi}_{12} - \dot{\varphi}_{13}) + M_r = 0
\end{aligned} \tag{2.1}$$

where

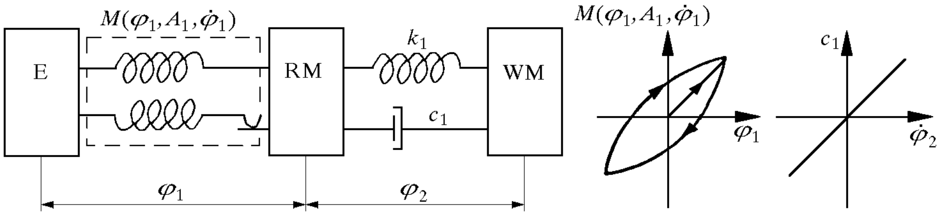

Fig. 2. Mechanical system with a non-linear hysteresis loop and linear viscotic damping reduced to two-degrees-of-freedom

I_1, I_2, I_3	–	mass moments of inertia of the driving and driven part, respectively
$\varphi_{11}, \varphi_{12}, \varphi_{13}$	–	angular displacements
M_z	–	clutch friction torque in a cycle represented by the structural hysteresis loop (Fig. 2), dependent on the relative angular displacement, its vibration amplitude and its sign of velocity, respectively
c_1	–	coefficient of viscous damping (Fig. 2)
M_r	–	resistance torque
$M(t) + M_m$	–	variable engine torque described by the constant average value of the nominal driving torque M_m and discrete torque $M(t)$ in the form of a harmonic excitation, i.e.

$$M(t) = M_0 \cos \omega t \tag{2.2}$$

and

M_0	–	amplitude of the excitation torque
ω	–	angular velocity of the excitation torque
t	–	time

and

$$M_z = \begin{cases} M(\varphi_1, A_1, \dot{\varphi}_1) & \text{for} \quad \rho < \rho_1 \\ M_T(\dot{\varphi}) & \text{for} \quad R \geqslant \rho > \rho_1 \end{cases} \tag{2.3}$$

Having used the results presented by Skup (2001), a limited radius sliding zone ρ_1, shown in Fig. 3, and $M = M(\varphi_1, A_1, \dot{\varphi}_1)$, shown in Fig. 2, were determined.

Thus,

$$M(\varphi_1, A_1, \dot{\varphi}_1) = \frac{1}{\sqrt{\eta_3}}\Big(\sqrt{\frac{A_1}{2}} + \sqrt{A_1 + \varphi \operatorname{sgn} \dot{\varphi}} \operatorname{sgn} \dot{\varphi} - \frac{\sqrt{2A_1}}{2} - \frac{\sqrt{2A_1}}{2} \operatorname{sgn} \dot{\varphi}\Big) \tag{2.4}$$

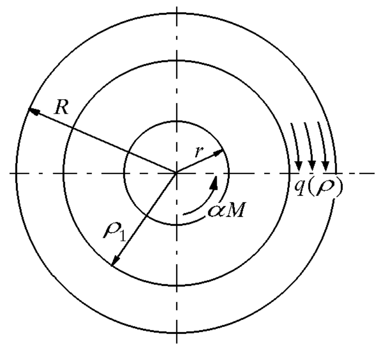

Fig. 3. Load distribution in the frictional pair

and

$$
\begin{array}{lll}
\nu = \dfrac{3}{2\pi\mu p R^3} & \rho_1 = r\sqrt[3]{1+\nu\alpha M} & 0 \leqslant \alpha \leqslant 1 \\
\eta_3 = \dfrac{\kappa_1\nu^2}{6} & \kappa_1 = \dfrac{2\delta(k_1+k_2)}{k_1k_2} & \delta = \dfrac{\mu p R}{6} \\
k_1 = Gh_1 & k_2 = Gh_2 &
\end{array}
\tag{2.5}
$$

where

η_3, α	–	nondimensional parameters
k_1, k_2	–	stiffness of discs
h_1, h_2	–	their thickness
μ	–	friction coefficient
p	–	pressure per unit area
r, R	–	internal and external radius of the discs
G	–	shear modulus
$M_T(\dot{\varphi})$	–	friction torque dependent on the sign of relative angular velocity.

The moment of friction in the friction clutch is described as below

$$
M_T(\dot{\varphi}) = 2\pi \int\limits_{\rho_1}^{R} p(\rho)\rho^2\mu(\dot{\varphi})\, d\rho
\tag{2.6}
$$

where ρ is the radius $(r \leqslant \rho \leqslant R)$, $\mu(\dot{\varphi})$ – variable value of the friction coefficient dependent on the relative angular velocity. The hysteresis loop described by (2.4) and (2.6) is shown in Fig. 4.

In the case of macro-slide of the collaborating discs and plunger $(\rho_1 = r)$, we obtain

$$
M_T(\dot{\varphi}) = \frac{2}{3}\pi p(R^3 - r^3)\mu(\dot{\varphi})
\tag{2.7}
$$

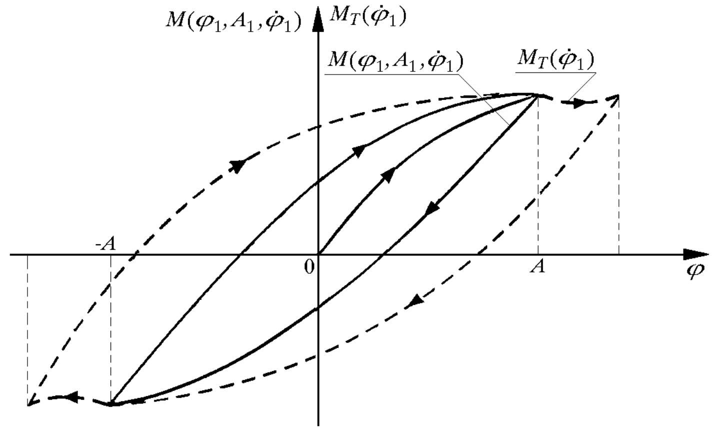

Fig. 4. Hysteresis loops: $M_T(\dot{\varphi})$, $M(\varphi_1, A_1, \dot{\varphi}_1)$ – moments of friction for kinetic and static friction

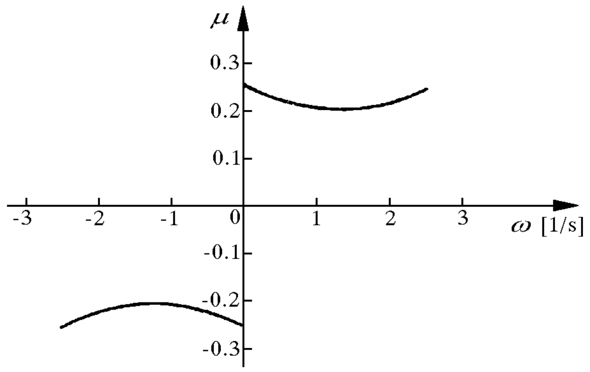

Fig. 5. Variation of the friction coefficient in function of relative speed of sliding discs

In the papers by Grudziński *et al.* (1992) Kołacin (1991), Pop and Stelter (1990), Skup (1998), theoretical studies were confirmed by experimental research. Therefore, variation of the friction coefficient $\mu(\dot{\varphi})$ shown in Fig. 5 can be determined in the following form:

$$\mu(\dot{\varphi}) = (a_1 - c_1\dot{\varphi}^2)\,\mathrm{sgn}\,\dot{\varphi} - b_1\dot{\varphi} + d_1\dot{\varphi}^3 \tag{2.8}$$

where a_2, b_2, c_2, d_2 are constant parameters. The numerical results were obtained for the following set of data for dry friction

$$\begin{array}{lll} a_2 = 0.25 & b_2 = 0.03 & c_2 = 0.02 \\ d_2 = 0.002 & \dot{\varphi} = \omega = 1\,\mathrm{rad/s} & \end{array} \tag{2.9}$$

3. The solution to equations of motion

Since we are interested in steady motion of the considered system, we assume $M_m = M_r$, which provides a uniform rotation of the undisturbed system.

Introducing new variables: $\varphi_1 = \varphi_{11} - \varphi_{12}$ and $\varphi_2 = \varphi_{12} - \varphi_{13}$ in forms of relative angles of torsion, we can reduce equations (2.1) to two second-order non-linear differential equations describing relative torsional vibration

$$\begin{aligned}
&\ddot{\varphi}_1 - c\dot{\varphi}_2 + f_1(\varphi_1, A_1, \dot{\varphi}_1) - m\varphi_2 - B = z\cos\omega t \\
&\ddot{\varphi}_2 + w\dot{\varphi}_2 + n\varphi_2 - \beta f_1(\varphi_1, A_1, \dot{\varphi}_1) - A = 0
\end{aligned} \tag{3.1}$$

where

$$\begin{array}{lll}
c = \dfrac{c_1}{I_2} & f_1(\varphi_1, A_1, \dot{\varphi}_1) = \dfrac{M_z}{I_{z1}} & m = \dfrac{k_1}{I_2} \\
k_1 = \dfrac{\pi G d_1^4}{32 l_1} & B = \dfrac{M_m}{I_1} & z = \dfrac{M_0}{I_1} \\
w = \dfrac{c_1}{I_{z2}} & n = \dfrac{k_1}{I_{z2}} & A = \dfrac{M_m}{I_3} \\
I_{z1} = \dfrac{I_1 I_2}{I_1 + I_2} & I_{z2} = \dfrac{I_2 I_3}{I_2 + I_3} & \beta = \dfrac{I_1}{I_1 + I_2}
\end{array} \tag{3.2}$$

Let the solution to the system of equations (3.1) be approximated by

$$\varphi_1 = A_1 \cos\theta_1 \qquad \varphi_2 = A_2 \cos\theta_2 \tag{3.3}$$

where

$$\theta_1 = \omega t - \phi_1 \qquad \theta_2 = \theta_1 - \phi_2 \tag{3.4}$$

and A_1, A_2, ϕ_1, ϕ_1 are all slowly varying functions of time t. Then

$$\begin{aligned}
\dot{\varphi}_1 &= \dot{A}_1 \cos\theta_1 + A_1\dot{\phi}_1 \sin\theta_1 - A_1\omega \sin\theta_1 \\
\dot{\varphi}_2 &= \dot{A}_2 \cos\theta_2 + A_2\dot{\phi}_2 \sin\theta_2 - A_2\omega \sin\theta_2
\end{aligned} \tag{3.5}$$

By analogy to Lagrange's method of variation of a parameter, it is permissible to propose the following

$$\begin{aligned}
\dot{A}_1 \cos\theta_1 + A_1\dot{\phi}_1 \sin\theta_1 = 0 \\
\dot{A}_2 \cos\theta_2 + A_2\dot{\phi}_2 \sin\theta_2 = 0
\end{aligned} \tag{3.6}$$

Thus

$$\begin{aligned}\ddot{\varphi}_1 &= \omega A_1\dot{\phi}_1\cos\theta_1 - A_1\omega^2\cos\theta_1 - \omega\dot{A}_1\sin\theta_1\\ \ddot{\varphi}_2 &= \omega A_2\dot{\phi}_2\cos\theta_2 - A_2\omega^2\cos\theta_2 - \omega\dot{A}_2\sin\theta_2\end{aligned} \tag{3.7}$$

Substituting equations (3.7) and $(3.5)_2$ into equations of motion (3.1) and using formulas (3.3), (3.4), (3.6), are arrives at

$$\begin{aligned}&\omega A_1\dot{\phi}_1\cos\theta_1 - A_1\omega^2\cos\theta_1 - \omega\dot{A}_1\sin\theta_1 + cA_2\omega\sin\theta_2 +\\ &\quad + f_1(A_1,\theta_1) - mA_2\cos\theta_2 - B = z\cos(\theta_1+\phi_1)\\ &\omega A_2\dot{\phi}_2\cos\theta_2 - A_2\omega^2\cos\theta_2 - \omega\dot{A}_2\sin\theta_2 - wA_2\omega\sin\theta_2 +\\ &\quad + nA_2\cos\theta_2 - \beta f_1(A_1,\theta_1) - A = 0\end{aligned} \tag{3.8}$$

Multiplying equation $(3.6)_1$ by $\omega\cos\theta_1$, equation $(3.8)_1$ by $\sin\theta_1$, then subtracting the sides and using formula (3.4), we obtain

$$\begin{aligned}&-A_1\omega^2\sin\theta_1\cos\theta_1 - \omega\dot{A}_1 + f_1(A_1,\theta_1)\sin\theta_1 - B\sin\theta_1 +\\ &-mA_2\cos\theta_2\sin(\theta_2+\phi_2) + cA_2\omega\sin\theta_2\sin(\theta_2+\phi_2) = z\sin\theta_1\cos(\theta_1+\phi_1)\end{aligned} \tag{3.9}$$

Since the variables A_1, A_2, ϕ_1 and ϕ_2 are assumed to be slowly varying, they remain essentially constant over one cycle of θ_1.

Thus equation (3.9) may be averaged over one cycle of θ_1, which gives

$$\begin{aligned}&-\omega\dot{A}_1 + \frac{1}{2}cA_2\omega\cos\phi_2 + \frac{1}{2\pi}\int\limits_0^{2\pi} f_1(A_1,\theta_1)\sin\theta_1\;d\theta_1 - \frac{1}{2}mA_2\sin\phi_2 =\\ &= -\frac{1}{2}z\sin\phi_1\end{aligned} \tag{3.10}$$

Multiplying equation $(3.6)_1$ by $\omega\sin\theta_1$, equation $(3.8)_1$ by $\cos\theta_1$, adding the sides, and using formula (3.4), gives

$$\begin{aligned}&\omega A_1\dot{\phi}_1 - A_1\omega^2\cos^2\theta_1 + cA_2\omega\sin\theta_2\cos(\theta_2+\phi_2) + f_1(A_1,\theta_1)\cos\theta_1 +\\ &-mA_2\cos\theta_2\cos(\theta_2+\phi_2) - B\cos\theta_1 = z\cos\theta_1\cos(\theta_1+\phi_1)\end{aligned} \tag{3.11}$$

Averaging equation (3.11) over one cycle of θ_1, gives

$$\begin{aligned}&\omega A_1\dot{\phi}_1 - \frac{1}{2}cA_2\omega\sin\phi_2 - \frac{1}{2}A_1\omega^2 + \frac{1}{2\pi}\int\limits_0^{2\pi} f_1(A_1,\theta_1)\cos\theta_1\;d\theta_1 +\\ &-\frac{1}{2}mA_2\cos\phi_2 = \frac{1}{2}z\cos\phi_1\end{aligned} \tag{3.12}$$

Similarly, multiplying equation $(3.6)_2$ by $\omega\cos\theta_2$, equation $(3.8)_2$ by $\sin\theta_2$, subtracting the sides, and using formula (3.4), yields

$$\begin{aligned}&\omega\dot{A}_2 + A_2\omega^2\sin\theta_2\cos\theta_2 + wA_2\omega\sin^2\theta_2 - nA_2\sin\theta_2\cos\theta_2 + \\ &+\beta f_1(A_1,\theta_1)\sin(\theta_1-\phi_2) + A\sin\theta_2 = 0\end{aligned} \tag{3.13}$$

With equation (3.13) averaged over one cycle of θ_1, we obtain

$$\begin{aligned}&\omega\dot{A}_2 + \frac{1}{2}wA_2\omega + \frac{\beta\cos\phi_2}{2\pi}\int\limits_0^{2\pi} f_1(A_1,\theta_1)\sin_1\;d\theta_1 + \\ &-\frac{\beta\sin\phi_2}{2\pi}\int\limits_0^{2\pi} f_1(A_1,\theta_1)\cos\theta_1\;d\theta_1 = 0\end{aligned} \tag{3.14}$$

Finally, multiplying equation $(3.6)_2$ by $\omega\sin\theta_2$, equation $(3.8)_2$ by $\cos\theta_2$, adding the sides, and using formula (3.4), gives

$$\begin{aligned}&\omega A_2\dot{\phi}_2 - A_2\omega^2\cos^2\theta_2 - wA_2\omega\sin\theta_2\cos\theta_2 + nA_2\cos^2\theta_2 + \\ &-\beta f_1(A_1,\theta_1)\cos(\theta_1-\phi_2) - A\cos\theta_2 = 0\end{aligned} \tag{3.15}$$

After averaging over one cycle of θ_1, equation (3.15) takes the following form

$$\begin{aligned}&\omega A_2\dot{\phi}_2 - \frac{1}{2}A_2\omega^2 + \frac{1}{2}nA_2 - \frac{\beta\cos\phi_2}{2\pi}\int\limits_0^{2\pi} f_1(A_1,\theta_1)\cos\theta_1\;d\theta_1 + \\ &-\frac{\beta\sin\phi_2}{2\pi}\int\limits_0^{2\pi} f_1(A_1,\theta_1)\sin\theta_1\;d\theta_1 = 0\end{aligned} \tag{3.16}$$

Steady-state equations (3.10), (3.12), (3.14) and (3.16) can be obtained when $\dot{A}_1 = \dot{A}_2 = \dot{\phi}_1 = \dot{\phi}_2 = 0$

When the following notations are introduced

$$\begin{aligned}S_1 &= \frac{1}{\pi}\int\limits_0^{2\pi} f_1(A_1,\theta_1)\sin\theta_1\;d\theta_1 \\ C_1 &= \frac{1}{\pi}\int\limits_0^{2\pi} f_1(A_1,\theta_1)\cos\theta_1\;d\theta_1\end{aligned} \tag{3.17}$$

equations (3.10), (3.12), (3.14) and (3.16) assume the following form

$$
\begin{aligned}
&-S_1 + mA_2 \sin\phi_2 - cA_2\omega\cos\phi_2 = -z\sin\phi_1 \\
&-A_1\omega^2 + C_1 - mA_2\cos\phi_2 - cA_2\omega\sin\phi_2 = z\cos\phi_1 \\
&wA_2\omega + \beta S_1\cos\phi_2 - \beta C_1\sin\phi_2 = 0 \\
&(n-\omega^2)A_2 - \beta C_1\cos\phi_2 - \beta S_1\sin\phi_2 = 0
\end{aligned}
\tag{3.18}
$$

The variable ϕ_1 may be eliminated from the foregoing equations by squaring and adding equations $(3.18)_{1,2}$. This gives

$$
(S_1 - mA_2\sin\phi_2 + cA_2\omega\cos\phi_2)^2 + (C_1 - A_1\omega^2 - cA_2\omega\sin\phi_2 - mA_2\cos\phi_2)^2 = z^2
\tag{3.19}
$$

Equations $(3.18)_{3,4}$ may be rewritten in the following form

$$
\begin{aligned}
\sin\phi_2 &= \frac{A_2[S_1(n-\omega^2) + w\omega C_1]}{\beta(C_1^2 + S_1^2)} \\
\cos\phi_2 &= \frac{A_2[C_1(n-\omega^2) - w\omega S_1]}{\beta(C_1^2 + S_1^2)}
\end{aligned}
\tag{3.20}
$$

In order to determine the amplitude A_2, the second equation has to be formulated by means of squaring and adding the sides of equations (3.20). Performing the indicated operations and rearranging the equations, are obtains

$$
A_2^2 = \frac{\beta^2(S_1^2 + C_1^2)}{[(n-\omega^2)^2 + w^2\omega^2]}
\tag{3.21}
$$

Equations (3.20) can be used to eliminate the variable ϕ_2 from equation (3.19). Therefore, substituting equations (3.20) and (3.21) into equation (3.19) and rearranging them, gives

$$
\beta z^2 = (C_1^2 + S_1^2)(\alpha_1 - \alpha_4) + A_1(\alpha_2 S_1 + \alpha_3 C_1) + \alpha_5 A_1^2
\tag{3.22}
$$

where

$$
\begin{aligned}
x &= \frac{\beta^2}{[(n-\omega^2)^2 + w^2\omega^2]} & \alpha_1 &= \beta[1 + x(m^2 + c^2\omega^2)] \\
\alpha_2 &= 2x\omega^3[(n-\omega^2) - wm] & \alpha_3 &= 2\omega^2\{x[m(n-\omega^2) + \omega^2 w] - \beta\} \\
\alpha_4 &= 2x[\omega^2 cw - m(n-\omega^2)] & \alpha_5 &= \beta\omega^4
\end{aligned}
\tag{3.23}
$$

For $\dot{\varphi} = 0$, there appears a discontinuity yn $M(\varphi_1, A_1, \dot{\varphi}_1)$. To avoid this while integrating Eqs. (3.17), we confine our considerations to a single half-period (motion between two stops).

Thus, the integration interval (from 0 to 2π) of the right-hand terms of the above equations is divided into two sub-intervals: from 0 to π for negative $\mathrm{sgn}\,\dot{\varphi}_1$ and from π to 2π for positive $\mathrm{sgn}\,\dot{\varphi}_1$. Such a procedure, for instance, was adopted by Caughey (1960), Osiński (1998) and Skup (1998).

Therefore, after substituting formulas (2.4) and (2.7) into equations (3.17) by using formula (3.2) and subsequent integration, we obtain the following relationships after some transformations

$$
\begin{aligned}
C_1 &= \frac{1}{\pi}\int\limits_0^{2\pi} f_1(A,\theta)\cos\theta\, d\theta = \\
&= \frac{1}{\pi I_{z1}}\Big\{\int\limits_0^{\pi}[M(\varphi_1, A_1, \dot{\varphi}_1) + M_T(\dot{\varphi})]\cos\theta\, d\theta_{\downarrow \mathrm{sgn}\,\dot{\varphi}<0}\Big\} + \\
&+ \frac{1}{\pi I_{z1}}\Big\{\int\limits_{\pi}^{2\pi}[M(\varphi_1, A_1, \dot{\varphi}_1) + M_T(\dot{\varphi})]\cos\theta\, d\theta_{\downarrow \mathrm{sgn}\,\dot{\varphi}>0}\Big\} = \frac{8\sqrt{A_1}}{3\pi I_{z1}\sqrt{2\eta_3}}
\end{aligned}
\tag{3.24}
$$

$$
\begin{aligned}
S_1 &= \frac{1}{\pi}\int\limits_0^{2\pi} f_1(A,\theta)\cos\theta\, d\theta = \\
&= \frac{1}{\pi I_{z1}}\Big\{\int\limits_0^{\pi}[M(\varphi_1, A_1, \dot{\varphi}_1) + M_T(\dot{\varphi})]\sin\theta\, d\theta_{\downarrow \mathrm{sgn}\,\dot{\varphi}<0}\Big\} + \\
&+ \frac{1}{\pi I_{z1}}\Big\{\int\limits_{\pi}^{2\pi}[M(\varphi_1, A_1, \dot{\varphi}_1) + M_T(\dot{\varphi})]\sin\theta\, d\theta_{\downarrow \mathrm{sgn}\,\dot{\varphi}>0}\Big\} = \\
&= \frac{1}{\pi I_{z1}}\Big[4F\Big(\frac{2}{3}c_2 A_1^2\omega^2 - a_2\Big) - \frac{4\sqrt{A_1}}{3\sqrt{2\eta_3}}\Big]
\end{aligned}
$$

Finally, substituting equations (3.24) into equation (3.22) and (3.21) and using formulas (3.23), gives

$$
\begin{aligned}
& T_8A_1^8 + T_7A_1^7 + T_6A_1^6 - T_5A_1^5 + T_4A_1^4 + T_3A_1^3 + T_2A_1^2 + T_1A_1 + T_0 = 0 \\
& A_2^2 = \frac{x}{\pi^2 I_{z1}^2}\Big\{\frac{32A_1}{9\eta_3} + \Big[4F\Big(\frac{2}{3}c_2A_1^2\omega^2 - a_2\Big) - \frac{4\sqrt{A_1}}{3\sqrt{2\eta_3}}\Big]\Big\}
\end{aligned}
\tag{3.25}
$$

where

$$
\begin{aligned}
T_0 &= \beta^2 z^4 + \alpha_{18}(\alpha_{18} - 2\beta z^2) + \alpha_{14}^2 & T_5 &= 2(\alpha_{11}\alpha_{12} + \alpha_{10}\alpha_{13}) \\
T_1 &= 2[\alpha_{13}(\alpha_{18} - \beta z^2)] + \alpha_{14}\alpha_{16} & T_6 &= \alpha_{11}^2 + 2\alpha_{10}\alpha_{12} \\
T_2 &= \alpha_{18}^2 - 2\alpha_{12}(\beta z^2 - \alpha_{18}) + \alpha_{16}^2 + 2\alpha_{14}\alpha_{15} & T_7 &= 2\alpha_{10}\alpha_{11} \\
T_3 &= 2[\alpha_{12}\alpha_{13} + \alpha_{11}(\alpha_{18} - \beta z^2)] + \alpha_{15}\alpha_{16} & T_8 &= \alpha_{10}^2 \\
T_4 &= \alpha_{12}^2 + \alpha_{15}^2 + 2[\alpha_{11}\alpha_{13} + \alpha_{10}(\alpha_{18} - \beta z^2)]
\end{aligned}
\tag{3.26}
$$

and

$$
\begin{aligned}
\alpha_6 &= \frac{8Fc_2\omega^2}{3\pi I_{z1}} & \alpha_7 &= \frac{4Fa_2}{\pi I_{z1}} \\
\alpha_8 &= \frac{16F}{3\pi I_{z1}\sqrt{2\eta_3}} & \alpha_9 &= \frac{8}{3\pi I_{z1}\sqrt{2\eta_3}} \\
\alpha_{10} &= \alpha_1\alpha_6^2 - \alpha_4\alpha_6^2 & \alpha_{11} &= \alpha_2\alpha_6 \\
\alpha_{12} &= 2\alpha_6\alpha_7(\alpha_4 - \alpha_1) + \alpha_5 & \alpha_{13} &= (\alpha_1 - \alpha_4)(\alpha_8^2 + \alpha_9^2) - \alpha_2\alpha_7 \\
\alpha_{14} &= 2\alpha_7\alpha_8(\alpha_1 - \alpha_4) & \alpha_{15} &= 2\alpha_6\alpha_8(\alpha_4 - \alpha_1) \\
\alpha_{16} &= \alpha_3\alpha_9 - \alpha_2\alpha_8 & \alpha_{18} &= \alpha_1\alpha_7
\end{aligned}
\tag{3.27}
$$

Thus, the formulated steady-state problem has been reduced to a set of two equations, i.e. (3.25), with two unknown amplitudes A_1 and A_2.

Equation $(3.25)_1$ was solved by means of the Newton-Raphson Iterative Technique method. We had to choose one from the eight roots of equation $(3.25)_1$ which would satisfy the physical condition.

That root takes a specific value of the deformation amplitude in the examined system. For such a value of A_1, the value of A_2 was calculated with formula $(3.25)_2$ in function of the forced vibration frequency.

4. Numerical results

The following data has been assumed in the numerical calculations

$$
\begin{aligned}
&h_1 = 0.00125 \text{ m} && h_2 = 0.00103 \text{ m} && r = 0.050 \text{ m} \\
&M_0 = 20 \text{ Nm} && \mu = 0.21 && d = 0.035 \text{ m}
\end{aligned}
$$

$I_1 = 0.35$ kgm^2 $\qquad I_2 = 0.08$ kgm^2 $\qquad I_3 = 0.420$ kgm^2

$l = 0.25$ m $\qquad p = 1.2 \cdot 10^5$ N/m^2 $\qquad G = 8.1 \cdot 10^{10}$ N/m^2

$c_1 = 0.50$ Nms

On the basis of results of the numerical analysis, it has been found that all resonance curves do not start from zero but tend asomptically to zero in the superresonance range (Fig. 6 – Fig. 9).

The response curves are typical for the "soft" type of resonance (Fig. 6). The influence of the loading amplitude (Fig. 6), unit pressures (Fig. 7), viscotic damping (Fig. 8) and the internal radius (Fig. 9) on the process of vibration damping has been examined in the numerical calculations as well. Diagrams in Fig. 6 show that the maximal values of the amplitudes A_1 and A_2 in the first resonance are significantly higher than their maximal values in the second resonance.

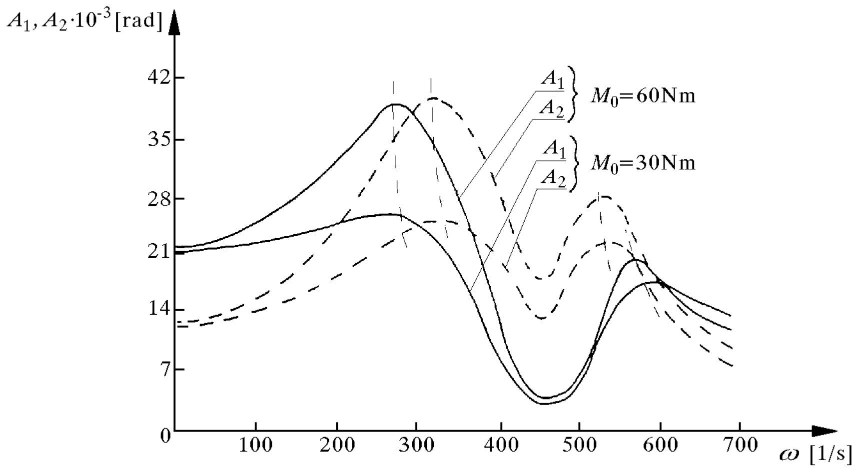

Fig. 6. Resonant curves for various amplitudes of the excitation torque M_0

There exists an optimal clamp of the clutch plates, where the resonance amplitudes in the first and second resonance reach the minimum (see Fig. 7). The reason for this is the increase of the sliding zone of the cooperating disc surfaces, which maximizes the loss of energy.

When the amplitude rises, the difference between the maximal values of the amplitudes A_1 in the first and second resonance grows a little, and the difference between the maximal values of the amplitude A_2 decreases a little.

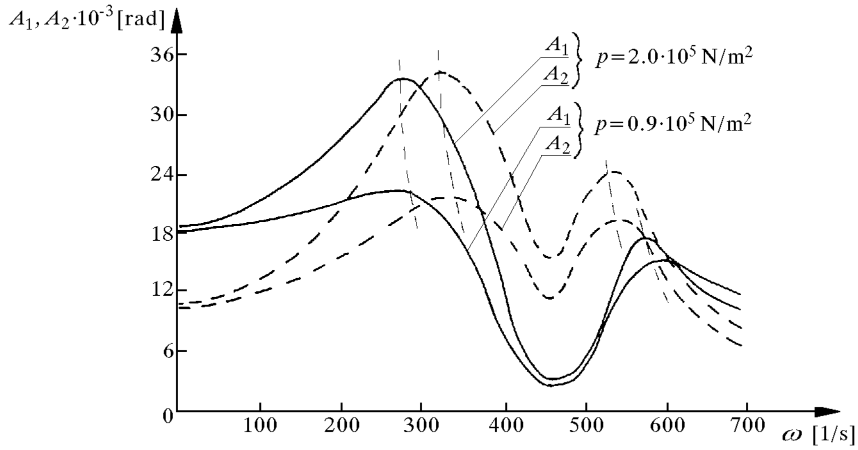

Fig. 7. Resonant curves for various values of the unit pressure p

The examined system has a "soft" frequency characteristic and damping diagram. An increase in the viscotic damping causes a decrease in the resonance amplitudes A_1 and A_2, particularly in the first resonance (Fig. 8).

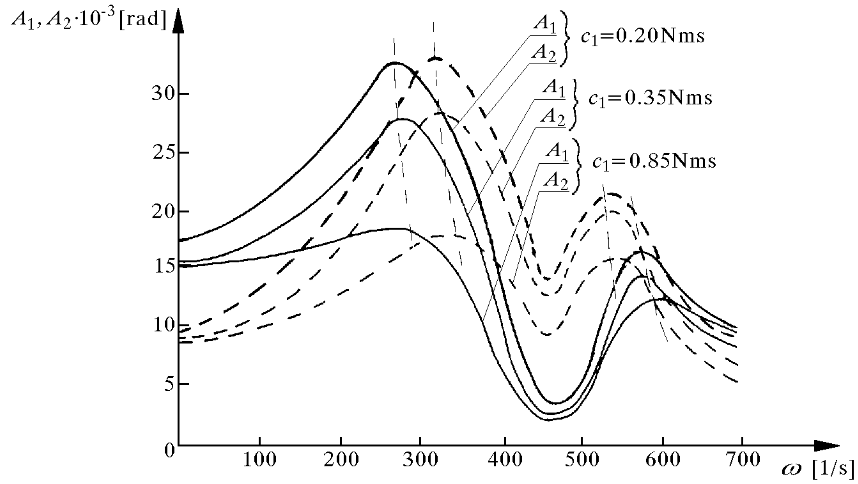

Fig. 8. Resonant curves for various values of the viscotic damping coefficient c_1

When the unit pressure increases, the sliding zone decreases, which entails weaker energy dissipation and decreased damping capability of the power transmission system. The less is the internal radius, the more visible becomes the damping vibration effect (Fig. 9).

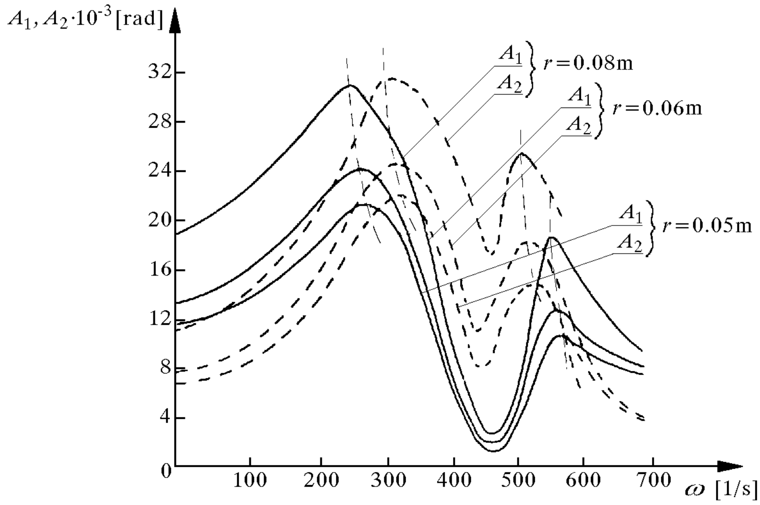

Fig. 9. Resonant curves for various values of the internal radius r of the discs

5. Concluding remarks

Structural friction between contacting surfaces of discs in the friction clutch causes increased performance of the examined system in terms of vibration damping. The author of the paper has carefully examined the effect of the most important parameters of the vibrating power transmission system with a friction clutch on resonant amplitudes.

On the basis of the obtained results, it has been found that all resonance curves start from a non-dimensional resonance amplitude and tend asymptotically to zero in the post-resonance zone. They also tend to assume a more smooth form in that zone. The damping effect is strongest for the optimal value of the friction force when the area of relative slide between the cooporating surfaces of discs is largest. The effects of structural friction and viscotic damping can be used in order to improve the design of dynamic systems.

Yet, it should be noted that vibration damping by friction clutches is considerably influenced by the following factors: amplitude of forcing, unit pressure, coefficient of viscous damping and internal radius of discs. The examined system has a "soft" frequency characteristic and attenuation diagram.

References

1. Buczkowski R., 1999, Statistical modeling of rough surfaces and finite element contact analysis, Rozprawa habilitacyjna, *Prace IPPT-PAN*, **3**

2. Buczkowski R., Kleiber M., 1997, Elasto-plastic interface model for 3D frictional orthotropic contact problems, *Int. Numer. Methods Eng.*, **40**, 599-619

3. Caughey T. K., 1960, Sinusoidal excitation of a system with bilinear hysteresis, *Trans. ASME*, **82**, 640-643

4. Gałkowski Z., 1981, Analysis of non-stationary processes in a dynamical system with structural friction, Ph.D. thesis, (original title in Polish: Badanie procesów niestacjonarnych układu dynamicznego z uwzględnieniem tarcia konstrukcyjnego), Warsaw University of Technology

5. Giergiel J., 1990, *Tłumienie drgań mechanicznych*, PWN, Warszawa

6. Goodman L.E., Klamp I.H., 1956, Analysis of slip damping, with reference to turbine-blade vibration, *Journal of Applied Mechanics, Transactions ASME*, **78**, 421-429

7. Grudziński K., Kissing W., Zapłata L., 1992, Untersuchung Selbsterregter Reibungsschwingungen mit Hilfe eines Numerischen Simulationsverfahrens, *Technische Mechanik*, **13**, 7-14

8. Kołacin T., 1971, Determination of friction characteristics of porous bearings based on measurements of parameters brought about by the friction, (original title in Polish: Wyznaczanie charakterystyk tarcia łożysk porowatych z pomiarów parametrów drgań wywołanych tarciem), Ph.D. thesis, Warsaw University of Technology, No. 1, pp. 41-60

9. Kosior A., Wróbel J., 1986, Test of influence the forced variance on dynamics system of a two-degree-of-freedom with hysteretic loop, *Books Sciences Rzeszów University of Technology, Mechanics*, **12**, 49-52

10. Osiński Z., 1986, *Tłumienie drgań mechanicznych*, PWN, Warszawa

11. Osiński Z., 1998, *Damping of Vibrations*, A.A. BALKEMA/Rotterdam/Brookfield, 1998

12. Pian T.H.H., 1957, Structural damping of a simple built-up beam with riveted joints in bending, *Journal of Applied Mechanics*, **24**, 35-38

13. Pietrzakowski M., 1986, Analysis of a simple system with structural friction by the space-time FEM, *XXII Symposium Vibrations in Physical Systems*, Błażejewko, 222-223

14. Popp K., Stelter P., 1990, Stick-slip vibrations and chaos, *Phil. Trans. R.Soc. Lond.*, **332**, 89-105

15. Skup Z., 1991,a Forced vibration of a nonlinear stationary system with a friction clutch, structural friction, being taken into consideration, *Engineering Transactions*, **39**, 69-87

16. Skup Z., 1991b, Vibration of a system with friction clutch with consideration of structural friction due to a random process, *Nonlinear Vibrations Problems*, **24**, 195-209

17. Skup Z., 1998, Wpływ tarcia konstrukcyjnego w wielotarczowym sprzęgle ciernym na drgania w układzie napędowym, *Prace naukowe PW, Mechanika*, **167**

18. Skup Z., 2001, Analysis of frictional vibration damper with structural friction taken into consideration, *Machine Dynamics Problems*, **25**, 2, 103-114

19. Skup Z., 2003, Active and passive damping of vibrations by torsional damper during steady state motion of a power transmission system, *Journal of Theoretical and Applied Mechanics*, **41**, 1, 155-167.

20. Skup Z., 2004, Vibration damping in a power transmission system containing a friction clutch, *Mathematik and Mechanik*, PAMM, **4**, Issue 1, 111-121

21. Szadkowski A., Morford R.B., 1992, Clutch engagement simulation: engagement without throttle, *SAE Technical Paper Series*, **920766**, 103-116

22. Zboiński G., Ostachowicz A., 1997, A general FE algorithm for 3D incremental analysis of frictional contact problems of elastoplasticity, *Finite Elements in Analysis and Design*, **27**, 289-305

Tłumienie drgań w układzie napędowym zawierającym sprzęgło cierne

Streszczenie

Artykuł przedstawia rozważania teoretyczne procesu tłumienia drgań nieliniowych w układzie napędowym o trzech stopniach swobody ze sprzęgłem ciernym włączanym elektromagnetycznie. Przedmiotem rozważań jest ruch ustalony układu poddanego wymuszeniu harmonicznemu. Zagadnienie rozpatrywane jest przy założeniu stałego rozkładu nacisku pomiędzy współpracującymi powierzchniami tarcz ciernych. Uwzględniane jest tarcie konstrukcyjne, mały względny poślizg tarcz sprzęgła oraz liniowe tłumienie wiskotyczne. W przypadku poślizgu współczynnik tarcia nie jest

stały, a zależy od względnej prędkości powoli ślizgających się tarcz. Celem analizy jest zbadanie wpływu geometrycznych parametrów układu, obciążenia zewnętrznego, nacisku jednostkowego, wiskotycznego współczynnika tłumienia na krzywe rezonansowe i kąta przesunięcia fazowego dla drgań ustalonych. Równania ruchu badanego układu zostały rozwiązane metodą powoli zmieniających się parametrów (metoda Van der Pola) i metodą symulacji cyfrowej.

Manuscript received April 25, 2005; accepted for print July 7, 2005